

**SYNTHESIS OF LITHIUM TITANATE BY AUTO COMBUSTION METHOD AND STUDY OF ITS
DENSIFICATION BEHAVIOR WITH DIFFERENT BINDER CONCENTRATION**

*A Thesis Submitted in Partial Fulfillment of the
Requirements for the Degree of*

Bachelor of Technology

in

CERAMIC

ENGINEERING

by

Mr. Chandan Dash

(Roll No: 107CR026)



**DEPARTMENT OF CERAMIC ENGINEERING
NATIONAL INSTITUTE OF TECHNOLOGY, ROURKELA**

**SYNTHESIS OF LITHIUM TITANATE BY AUTO COMBUSTION METHOD AND STUDY OF ITS
DENSIFICATION BEHAVIOR WITH DIFFERENT BINDER CONCENTRATION**

*A Thesis Submitted in Partial Fulfillment of the
Requirements for the Degree of*

Bachelor of Technology

in

CERAMIC

ENGINEERING

by

Mr. Chandan Dash
(Roll No: 107CR026)

Supervisor:

Dr. Ranabrata Mazumder



**DEPARTMENT OF CERAMIC ENGINEERING
NATIONAL INSTITUTE OF TECHNOLOGY, ROURKELA**



NATIONAL INSTITUTE OF TECHNOLOGY

Rourkela, INDIA

CERTIFICATE

This is to certify that the thesis entitled “**SYNTHESIS OF LITHIUM TITANATE BY AUTO COMBUSTION METHOD AND STUDY OF ITS DENSIFICATION BEHAVIOR WITH DIFFERENT BINDER CONCENTRATION**” being submitted by **Mr. Chandan Dash**, roll no. **107CR026**, for the degree of **Bachelor of Technology in Ceramic Engineering** to the National Institute of Technology, Rourkela, is a record of bonafide research work carried out by him under my supervision and guidance. His thesis may be considered for the award of degree of Bachelor of Technology in accordance with the regulations of the institute.

The results embodied in this thesis have not been submitted to any other university or institute for the award of a Degree.

(Supervisor)

Dr. R Mazumder

Department of Ceramic Engineering
National Institute of Technology
Rourkela

ACKNOWLEDGEMENT

I would, really from the bottom of my heart, express my gratitude to Dr. Ranabrata Mazumder for introducing me to this topic and showing me the guiding light at every possible circumstance during the course of this project.

My gratitude is also towards all the faculty of Department of Ceramic Engineering. Pratihara sir, thank you for your able guidance, Bera sir, Bhattacharya sir, R. Sarkar sir, D.Sarkar sir, Nayak sir, Pal sir, and Chowdhury sir for helping me proceed in the right path.

I would also like to thank Mr. Bhabani Shankar Sahu for being there at every step of the way during course of this project. Really, this project wouldn't have been a success if you were not by my side. I would like to express my gratitude also to other M.Tech and PhD. Scholars of our department for their kind help and support.

Also if I don't thank Mr. P.K.Mohanty, Mr.G.Behera and others, it would be really unjust on my part because they had as much hand in the completion of this project as anyone else.

Lastly, but in no sense the least, I would like to thank my friends for helping, supporting and sometimes carrying me with them throughout this journey.

Chandan Dash

ABSTRACT

In the current work, the Li_2TiO_3 powder was synthesized through the novel auto-combustion method using cheaper precursor of titanium i.e. TiO_2 . The nitrate solution was prepared by using the sulphate route and citric acid was used as the fuel. Citrate- nitrate combustion reaction was carried out to produce fine Li_2TiO_3 powder. It was seen that the pellets can be effectively sintered at 900°C obtaining densities of around 90% of the theoretical density. Different amount of PVA binder was added viz. 3%, 5%, 7% to fabricate pellets which were then sintered at different temperatures i.e. 900°C for 6 hours, 1000°C for 4 hours and 1100°C for 2 hours to produce pellets. The densification behavior of these pellets was studied and it was concluded that the 3% PVA pellets had the highest density among the different samples. Thermal expansion and electrical conductivity was measured on the highly dense pellets.

LIST OF FIGURES

<i>Sl.No.</i>	<i>Figure</i>	<i>Page</i>
Fig. 1.1	The fusion reaction of deuterium and tritium.	3
Fig. 2.1	Crystal structure of Li_2TiO_3	12
Fig. 4.1	Schematic representation of preparation of $\text{TiO}(\text{NO}_3)_2$ solution	19
Fig. 4.2	Flow chart for preparation of Li_2TiO_3 powder	20
Fig. 4.3	Photographs of citrate-nitrate solution	21
Fig. 5.1	XRD of Li_2TiO_3 with C/M=1 raw combustion powder and powder calcined (600°C)	27
Fig. 5.2	The dilatometric shrinkage curve	28
Fig. 5.3	The Bulk densities (relative) of Li_2TiO_3 at different sintering temperatures	29
Fig.5.4	SEM micrograph of Li_2TiO_3 sintered at 900°C (a) as cut and polished surface (b) polished surface	30
Fig. 5.5	The Thermal expansion behaviour of Li_2TiO_3 pellet sintered at 900°C for 6 hours.	31
Fig.5.6	Temperature dependence of AC conductivity of Li_2TiO_3 pellets (1000°C for 4 hours)	32

LIST OF ABBREVIATIONS

<i>Sl.No.</i>	<i>Abbreviation</i>	<i>Full Form</i>
1	Li_2TiO_3	Lithium Titanium Oxide
2	PVA	Poly Vinyl Alcohol
3	XRD	X-Ray Diffraction
4	SEM	Scanning Electron Microscope

CONTENTS

CERTIFICATE.....	I
ACKNOWLEDGEMENT.....	II
ABSTRACT.....	III
LIST OF FIGURES AND ABBREVIATIONS.....	IV
CHAPTER 1: INTRODUCTION.....	1
1.1 Introduction.....	2
1.2 Fusion reactions.....	2
1.3 Lithium bearing ceramics for Tritium production.....	4
1.4 Different kinds of breeder materials and their properties.....	4
CHAPTER 2: LITERATURE REVIEW.....	4
2.1 Synthesis and sintering of Breeder Materials.....	5
2.2 Binders.....	9
2.3 Crystal structure of Li_2TiO_3	11
2.4 Properties of Li_2TiO_3	12
CHAPTER 3: OBJECTIVE.....	15
CHAPTER 4: EXPERIMENTAL PROCEDURE AND CALCULATION.....	17
4.1 Powder synthesis	18
4.2 Preparation of $\text{TiO}(\text{NO}_3)_2$ solution and its estimation.....	18
4.3 Combustion Synthesis of Li_2TiO_3	20
4.4. Powder Characterization	21

CHAPTER 5: RESULTS AND DISCUSSION.....	26
5.1 Phase analysis	27
5.2 Shrinkage Characteristics	28
5.3 Densification.....	29
5.4 Microstructures of the pellets.....	30
5.5 Thermal Expansion.....	31
5.6 Electrical conductivity.....	32
CHAPTER 5: CONCLUSIONS AND SCOPE FOR FUTURE WORK.....	34
REFERENCES.....	36

CHAPTER 1

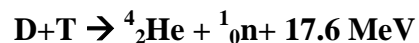
INTRODUCTION

1.1 Introduction:

There are about 436 nuclear reactors present in the world today, which mainly rely on fission reactions to produce energy. Nuclear fission can be defined as the splitting of heavy atomic nuclei, especially the very heavy ones like Uranium and Plutonium, to smaller nuclei thereby releasing energy [1]. However, there is an alternative method to produce energy through the process of nuclear fusion. Basically when two or more very light unstable nuclei come in contact, they combine to form a heavier stable nuclei with the release of a huge amount of energy. This is the basis of the nuclear fusion reactions and we get a process which can provide a clean, sustainable energy for the increasing needs of mankind.

1.2 Fusion reactions:

It is quite interesting to note that the energy produced in the sun and other stars is due to nuclear fission of hydrogen and helium. The easiest fusion reaction to achieve is that between deuterium and tritium [2]. In this reaction, Deuterium (D) and Tritium (T) fuse to form an alpha particle (Helium nuclei), a neutron and 17.6 MeV of energy [3].



The two newly formed particles take the released energy in the inverse proportion of their masses. So what this means is that the released neutron takes 80% of the energy and since it is unaffected by any magnetic fields, they are emitted in all directions. These neutrons are how the energy leaves the fusion chamber. Most of these neutrons leave the reactor on its outer edge and come to rest in a component preferably called as “the blanket”. The blanket contains material which can slow down the neutrons and get heated up in the process. This heat is then transferred to a medium like steam or high pressure Helium. This hot & high pressure gas is then used to

drive an electricity generating turbine. Now lithium is included in most of the blankets. The advantage of using Lithium is that when it comes in contact with the fast moving neutrons, they form Tritium, which is one of the fuels in the fusion reaction, thereby enabling the power plant to produce one component in situ.

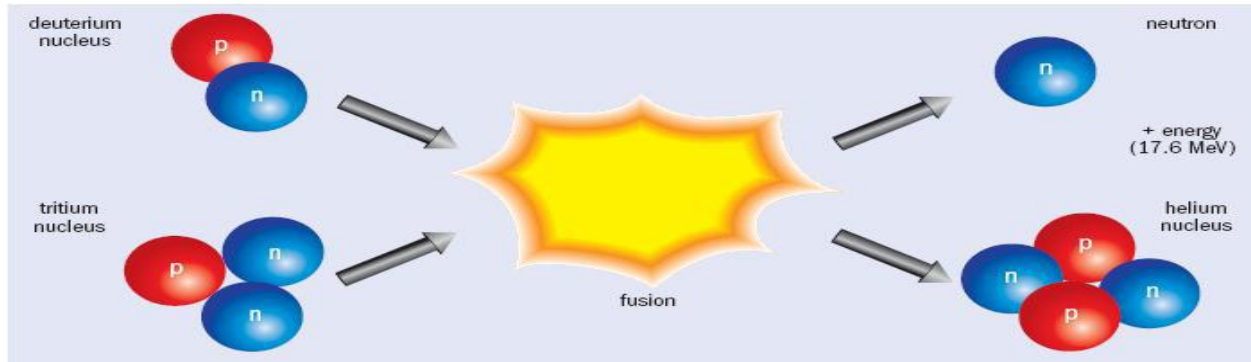
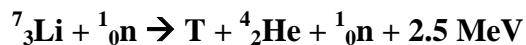
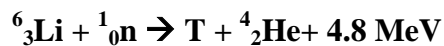


Fig. 1.1 The fusion reaction of deuterium and tritium.

However, the continuous operation of this power plant requires a continuous supply of the raw material i.e. Deuterium and Tritium into the reactor chamber. Procuring Deuterium is quite easy as it can be readily found in heavy water, and as earth contains about 10^{13} metric tons of Deuterium, one can say that there is quite an infinite supply.

But Tritium is quite rarely occurring in nature (roughly $10^{-16}\%$ of total H_2 present) and obtaining it in sufficient quantity to be a fuel is a tedious job. However, tritium can be produced from Lithium by some nuclear reactions.



1.3 Lithium bearing ceramics for Tritium production:

The interest in the use of Lithium based materials for use in breeder reactors has been on an increase since the 1970s. Ceramic Lithium materials are generally preferred because of their excellent characteristics in severe operating conditions of high temperatures and intense neutron fluxes. The Lithium based ceramics which have been considered as candidates for their use in D-T fusion reactors of ITER test blanket module (TBM) for DEMO reactors are Li_2O , $\gamma\text{-LiAlO}_2$, Li_4SiO_4 , Li_2ZrO_3 , and Li_2TiO_3 [4-7].

The requisite properties of a breeder material are:

- Breed and release Tritium,
- Physical and chemical stability should be adequate at high temperatures,
- The compatibility with other components of the blanket should be optimum,
- Adequate irradiation behavior should be exhibited.

As the Lithium based ceramics show overall ideal properties, they are the prime candidates in the fabrication of the fusion reactor blankets.

1.4 Different kinds of breeder materials and their properties:

The Lithium based ceramics like Li_2O , $\gamma\text{-LiAlO}_2$, Li_4SiO_4 , Li_2ZrO_3 , and Li_2TiO_3 are candidates for their use in D-T fusion reactors of ITER test blanket module (TBM) for DEMO reactors [4-7], [8-13].

Lithium Titanium Oxide (Li_2TiO_3):

- It has good Tritium release properties [10-13] along with better thermal and chemical stability, better thermal conductivity and very less reactivity with moisture.
- It also bonds well with other components of the blanket.

CHAPTER 2

LITERATURE REVIEW

2.1. Synthesis and sintering of Breeder Materials:

Various researchers synthesized Lithium Titanium oxide (Li_2TiO_3) by different methods. Basically, different synthesis routes have different costs, powder properties and different applications. The starting precursors used in each method usually determine the size of the particles which intern determines the properties and usability of the material.

The different methods for the synthesis can be divided into two groups:

- The solid state method,
- The chemical solution based method.

The solid state method involves grinding the precursors, generally in their oxide or carbonate forms, in hand mixing or in a high energy ball milling. However, the chemical solution based methods involve many a processes like combustion synthesis, sol-gel synthesis, co-precipitation technique, and soft solution processing.

2.1.1. The Solid state route:

Wu et al. [14] prepared Li_2TiO_3 by the solid state method. They took appropriate amounts of Li_2CO_3 (A.R.) and TiO_2 (A.R.) powders with the ratio of $\text{Li}/\text{Ti}=2$. Planetary ball milling was carried out for 4 hours with ethyl alcohol as the milling medium. The precursors were dried and calcined at 700°C for 4 hours in normal air atmosphere to obtain Li_2TiO_3 . Pebbles were fabricated, through the wet chemical method, which were sintered at 1050°C for 3 hours.

2.1.2. Synthesis of Li_2TiO_3 by solution route:

Chemical methods usually produce better homogenization of the particles at the molecular and atomic levels which produce better properties like submicron sized particles, low temperature calcination requirement etc. however, the actual properties of the powder depend on which route is chosen.

2.1.2.1. Polymer solution technique:

This technique is used to obtain nano-sized powders. Organic compounds like PVA (polyvinyl alcohol), PEG (polyethylene glycol) etc. are used as polymer carriers which make the soft solution processing easier. The segregation of metal ions in the solution is hindered by use of large chain polymers which help in proper homogenization [15, 16].

Jung et al. [17] worked on this method to produce Li_2TiO_3 . The precursors he used were Titanium (IV) iso-propoxide [$\text{Ti}(\text{OC}_3\text{H}_7)_4$], Lithium nitrate (LiNO_3) and ethylene glycol (EG), with a 1:4 metal to EG ratio. Around 70 nm sized porous particles were obtained which showed about 90% density when sintered at 1100°C for 2 hours.

2.1.2.2. The Organic-Inorganic solution technique:

Lee S.J. [18] produced Li_2TiO_3 by an organic-inorganic solution route where Titanium iso-propoxide [$\text{Ti}(\text{OC}_3\text{H}_7)_4$] and lithium nitrate (LiNO_3) were dissolved in the liquid-type ethylene glycol without any precipitation. The dried precursor gel showed crystalline Li_2TiO_3 at temperatures as low as 300°C and had a soft porous structure which was easily ground to obtain 0.2 μm particle size. Also a 91% of TD was achieved when sintered at 1200°C for 2 hours. A significant densification was observed between 800 - 1100°C .

2.1.2.3. Solution combustion synthesis:

The advantages of using the solution combustion technique are:

- the products of combustion synthesis are highly reactive,
- they contain minimum levels of impurities,
- they can be prepared rapidly,
- they normally, do not require specialized equipment for their preparation.

Precursors are generally prepared from an aqueous solution of the metal nitrates and an organic compound such as citric acid, carboxylate azides, urea or glycine [19-22].

Sinha et al. [23] worked on a single-step solid-liquid combustion process with hydrated TiO_2 and LiNO_3 to produce Li_2TiO_3 . However, the XRD analysis showed many unwanted phases which were produced due to the inhomogeneity in the solution mixture as complete dissolution of TiO_2 was very difficult. 90% density can be achieved after sintering to 1150°C , but the fracture surface shows huge amounts of entrapped pore which is detrimental.

Jung et al. [24, 25] synthesized Li_2TiO_3 by Glycine-nitrate auto-combustion technique where the titanium source was Ti-nitrate solution, prepared by hydrolyzing TiCl_4 followed by dissolving precipitate of Ti-hydroxide in HNO_3 . Other fuels like urea and citric acid were also studied. The particle size obtained was around 30 nm, and it showed 85% relative density when sintered at 1100°C for 4 hours. Later, pebbles of Li_2TiO_3 were developed by dry rolling granulation process (DRGP).

Cruz et al. [26] produced Li_2TiO_3 by combustion synthesis by using LiOH and TiO_2 and urea as the precursors in different molar ratios (2:1:3 and 3:1:3). It was observed that there is no significant advantage of this method than the conventional combustion method; the only advantage being reduction in the synthesis time period. However, on the downside, the product had a lot of

carbonaceous impurities. Also, the LiOH needed to be used in excess to compensate for the loss of Li sublimated during the ceramic production.

2.2. Binders:

2.2.1. PVA (poly vinyl alcohol):

Binders are often added in ceramic systems which involve drying of slurries followed by dry-pressing. The addition of these binders is necessary to impart the required cohesive strength to the sprayed granules [27], thereby imparting the free flowing properties [28]. Also, the binders can improve the strength of the green compacts, although they may have an effect on the relative densities [29]. Therefore the binders must carefully be selected so that they impart the requisite properties without causing any microstructural defects in the ceramic bodies during debinding [30].

Poly vinyl alcohol (PVA) is largely used as binder in the dry pressed bodies [31]. PVA is prepared by alkaline or acidic hydrolysis of poly vinyl acetate that usually leaves a small amount of acetate behind. This acetate helps in stabilizing the polymers by preventing the de-polymersization reaction [32].

2.2.2. Binder Removal:

The term binder removal or debinding refers to the removal of binders as well as other organic additives, like plasticizers, dispersants, and lubricants, from the green body. The mass transport processes responsible for binder removal involve liquid or gas flow; and thus the number of ways of removing the binder from the green body is limited. In general debinding can be accomplished by three methods:

A) Extraction by capillary flow into a porous surrounding material,

B) Solvent extraction,

C) Thermal decomposition.

However the most commonly used method is the thermal decomposition or simply referred to as binder burnout or thermal debinding.

In thermal debinding, the binder is removed as a vapor by heating at ambient temperatures in an oxidizing or non-oxidizing atmosphere, or under partial vacuum. The process is influenced by both chemical and physical factors. Chemically, the composition of the binder and the atmosphere determine the decomposition temperature and the decomposition products. Physically, the removal of the binder is controlled by heat transfer into the body and mass transport of the decomposition products out of the body.

In general, for a thermoplastic binder, thermal debinding can be roughly divided into three stages.

Stage 1 involves the initial heating of the binder to a point where it softens (~ 150 to 200⁰C) chemical decomposition and binder removal are negligible in this stage, but the occurrence of several other processes like shrinkage, deformation, and bubble formation can seriously affect the ability to control the shape and structural integrity of the body. Shrinkage occurs by a rearrangement process as the particles as the particles try to achieve a denser packing. Deformation is enhanced by lower particle packing, higher binder content, and lower melt viscosity. Bubble formation results from the decomposition of the binder as well as from the residual solvent, dissolved air, or air bubbles trapped within the green body during forming, and it provides a possible source of failure during the thermal binding [33].

In stage 2, typically covering a temperature range of 200-400⁰C, most of the molten binder is removed by evaporation. If the molten binder has sufficient, appreciable capillary flow of the

binder can accompany the evaporation process. Evaporation of low-molecular-weight binders can occur readily in inert atmospheres such as nitrogen or argon. High-molecular-weight polymers can neither flow nor evaporate until they have been degraded to low-molecular-weight segments.

In stage 3, the small amount of binder still remaining in the body is removed by evaporation and decomposition at temperatures above 400°C. Binder removal is facilitated by the highly porous nature of the body, but a small amount of carbon residue remains which is effectively removed when temperatures of more than 600°C are reached.

It is essential to achieve some balance between the time of debinding and the prevention of flaws during debinding. Normally this can be achieved by controlling the heating the cycle. A very low heating rate makes the thermal debinding process time consuming, whereas a high heating rate leads to bubble formation, rapid melting of binder and distortion of the body.

However, the decomposition of the polymeric binder in a ceramic green body is more complex than a pure binder. Details studies of powder and atmosphere effects on the binder burnout and decomposition chemistry of ceramic green bodies containing a single binder have been performed by Masia et.al. [34].

2.3. Crystal structure of Li_2TiO_3 :

Lang et al. [35] described the structure of Li_2TiO_3 as iso-structural with Li_2SnO_3 , which intern is a derivative of the rock-salt NaCl structure.

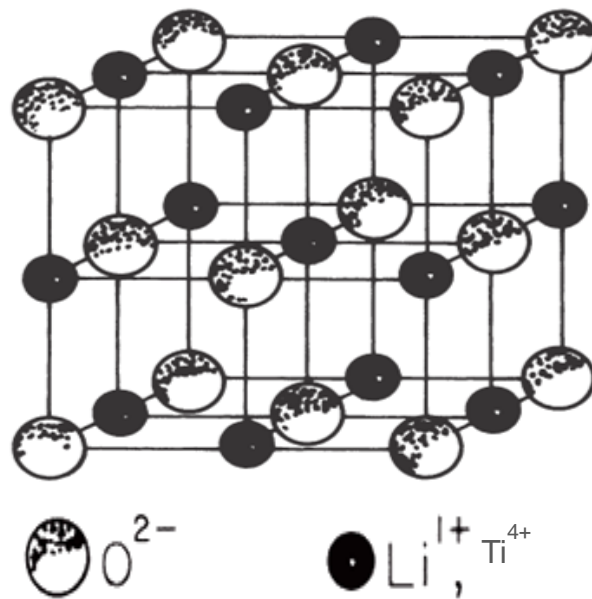


Fig. 2.1 Crystal structure of Li_2TiO_3

The monoclinic structure of Li_2TiO_3 is a result of the reorientation of the NaCl unit cell. In the cation sites of the NaCl structure, Li^+ and Ti^{4+} are randomly distributed. As it is iso-structural with Li_2SnO_3 , it is proposed that two types of layer structure exists; one composed of Lithium occupied octahedral voids and the other composed of Lithium and Titanium occupied octahedral voids, in 1:2 ratio, stacked alternately perpendicular to the a-b plane [36].

In case of Li_2TiO_3 , all the octahedral edges are shared between two Ti^{4+} , two Li^+ , or one Ti^{4+} and one Li^+ . The mean distances between the ions for each of the three categories takes different values, showing that the cation repulsion is chiefly responsible for the distortion in the rock-salt structure [35, 37].

2.4. Properties of Li_2TiO_3 :

2.4.1. Electrical Conductivity behavior:

Fehr et al. [38] investigated the conductivity of Li_2TiO_3 specimens having different microstructure and came to a conclusion that the difference in microstructure is the cause of the impedance

spectra change. So, samples were prepared in oxidizing as well as reducing atmospheres, which showed that the anomalies obtained at 880 K DC conductivity were due to the presence of high temperature cubic phase of Li_2TiO_3 .

Noda et al. [39] suggest that the tritium ion is in the valence state of T^+ and is assumed to be bound with the oxygen ions. The T^+ ions migrated by jumping from one oxygen lattice to the other. In such a migration process, the tritium ion must overcome the barrier of electrostatic repulsion due to lithium ions. Since the lithium ion is considered to migrate through vacancy mechanism, the lithium ion diffusion causes frequent replacement of ion sites by ion vacancy. Hence, the repulsive force decreases and the tritium can easily migrate. So, the conclusion that was reached was higher is the lithium ion conductivity, higher will be the tritium diffusion.

2.4.2. Thermal properties:

The thermal conductivity is one of the most important properties for materials used as conducting materials. The effective thermal conductivity depends on a variety of factors like the size and density of pellets, surface conditions, packing fraction, gas composition, gas pressure, gas flow rate etc.

Davis et al. [40] studied the thermal diffusivity of the commercially available Li_2TiO_3 powder. The tests were done between 300-1000 K by the laser flash technique. It was observed that the conductivity decreased from 3-2.2 W/mK in between 425-600 K but increased again to about 2.6 W/mK at 1000 K. This in conductivity can be attributed to the increase in the heat capacity beyond 600 K.

Saito et al. [41] studied the dependence of density and thermal hysteresis on the thermal conductivity, specific heat and thermal expansion of the Li_2TiO_3 pellets from room temperature to

1100 K. Thermal hysteresis was observed neither in the heating cycle nor in the cooling cycle, thereby arising at a conclusion that Li_2TiO_3 is thermally stable from room temperature to 1100 K.

Abou-Sena et al. [42] studied the effective thermal conductivity of a Li_2TiO_3 pebble bed as a function of the average bed temperature. 1.7-2.0 mm diameter pebbles were taken in the bed with a 61% packing density. Helium at atmospheric pressure was used as a filling gas. The tests showed that the conductivity decreased from 1.40 to 0.94 W/mK as the temperature increased from 50-500°C.

CHAPTER 3

OBJECTIVE

The objectives of this project are:

- Synthesis of Li_2TiO_3 through a novel solution auto-combustion method with the help of cheaper source of Ti (e.g. TiO_2) rather than expensive ones like TiCl_4 or Ti isopropoxide.
- To study the densification characteristics of Li_2TiO_3 pellets by sintering at three different temperatures (900, 1000, 1100°C) with the addition of different amounts (3, 5, 7 wt. %) of PVA binder.
- Thermal expansion and electrical conductivity measurements on the highly dense samples.

CHAPTER 4

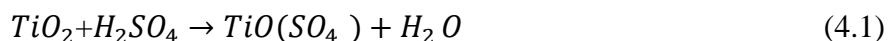
EXPERIMENTAL WORK

4.1 Powder synthesis:

Li_2TiO_3 powder has been synthesized through the solution combustion synthesis technique. Generally citric acid, urea, glycine etc. are used as the organic fuel and nitrates of different metals are used as the oxidants. The fuel has dual role, it helps in complex formation with the metal ions and finally, on decomposition and oxidation releases enormous amount of heat. The combustion may be associated with or without flame, and the flame temperature can be varied by varying amount of fuel and oxidizer taken, sometimes pH of the precursor solution. In the present work, Li_2TiO_3 powder has been synthesized by taking the starting precursor as Li_2CO_3 for lithium source and Ti-nitrate ($\text{TiO}(\text{NO}_3)_2$) solution. As $\text{TiO}(\text{NO}_3)_2$ was not commercially available, it was prepared using precipitation technique. The different experimental techniques used during the present study have been discussed below:

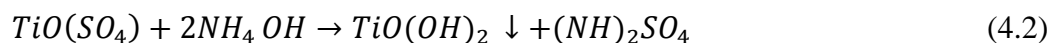
4.2 Preparation of $\text{TiO}(\text{NO}_3)_2$ solution and its estimation:

Titanium dioxide (TiO_2) is generally insoluble in mineral acid, however TiO_2 reacts with the sulphuric acid (H_2SO_4) and forms titanium sulphate. The formation of $\text{TiO}(\text{SO}_4)$ can be enhanced with the addition of ammonium sulphate $(\text{NH}_4)_2\text{SO}_4$. The preferred temperature was reported to be 80-90°C. Weighed amount of TiO_2 [Merck], and $(\text{NH}_4)_2\text{SO}_4$ [Merck], were mixed with concentrated H_2SO_4 [Merck] and this suspension was heated on hot plate with constant and vigorous stirring until a clear solution was obtained. The dissolution reaction may be written as:



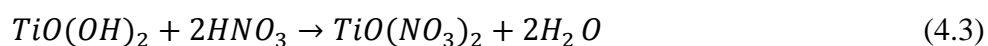
The solution was then diluted with addition of distilled water in an ice bath; since the acid-water reaction is highly exothermic, it may lead to precipitation. Ammonium hydroxide (NH_4OH)

[Merck] was added to chilled solution with constant stirring, wherein a white precipitate was formed. The possible reaction for the formation of precipitate may be written as



The precipitate was washed repeatedly with distilled water to make it sulphate free. Then, the washed white precipitate was dissolved in dilute nitric acid (HNO_3) [Merck], ($HNO_3: H_2O = 1:1$).

The possible reaction may be written as



Thus, the $TiO(NO_3)_2$ solution was prepared for the present study. TiO_2 content of the $TiO(NO_3)_2$ solution thus prepared has been estimated using gravimetric technique. The schematic flow chart of titanium nitrate solution preparation was shown in Fig. 4.1.

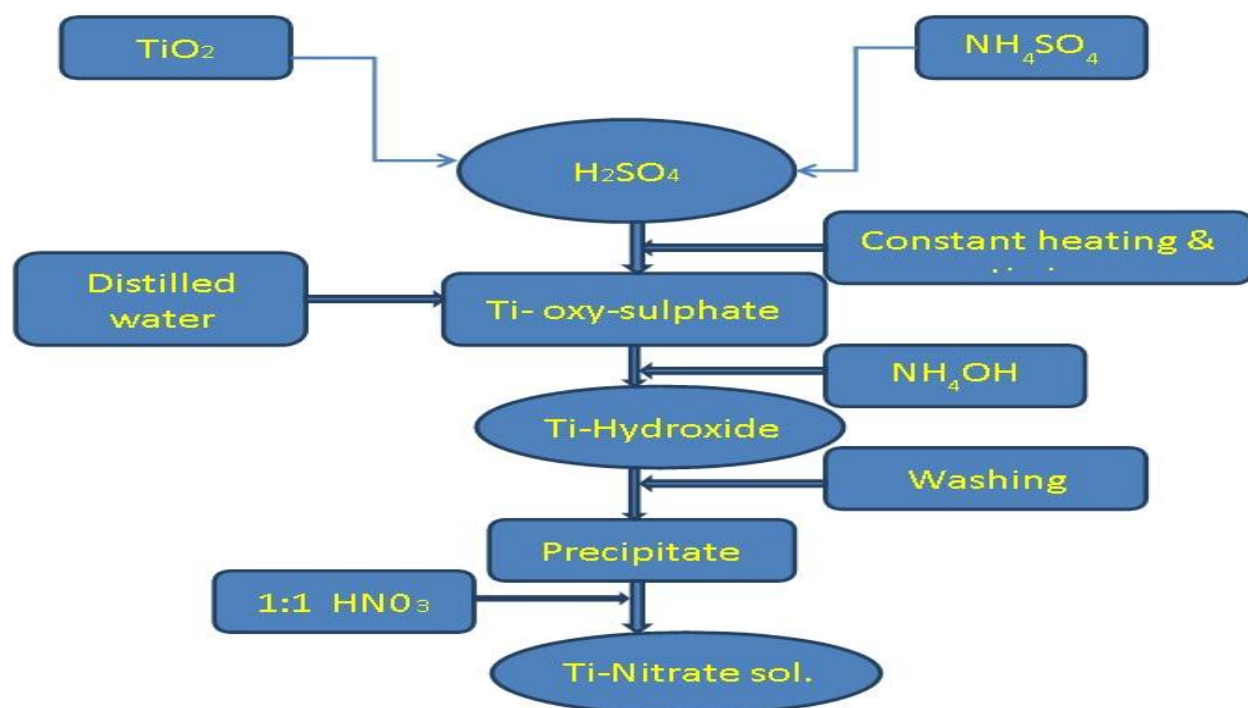


Fig. 4.1 Schematic representation of preparation of $TiO(NO_3)_2$ solution

4.3 Combustion Synthesis of Li_2TiO_3 :

The starting precursors for the preparation of Li_2TiO_3 taken were Lithium carbonate (Qualigens, 98.5%), titanium oxy-nitrate and citric acid (CA, Merck, 99 %). Citric acid plays the role of fuel as well as complexing agent. Citric acid ($\text{C}_6\text{H}_8\text{O}_7$) has three carboxylic and one hydroxyl group for coordinating to metal ions and therefore prevents precipitation or phase segregation, thus providing an intimate blending among constituent ions [43]. The molar ratio of the citrate to metal was kept at 1 and pH of the starting solution was at 1.

Stoichiometric amount of Li_2CO_3 , $\text{TiO}(\text{NO}_3)_2$ were mixed along with citric acid and heated at 80-100°C with constant stirring on hot plate. The schematic flow chart of sample preparation was shown in Fig. 4.2. The combustion is slow and flameless as can be seen in Fig.4.3 (a). The burnt powder was calcined at 600°C for 2 hours to get better crystallization and finally, ground to get the Li_2TiO_3 breeder powder.

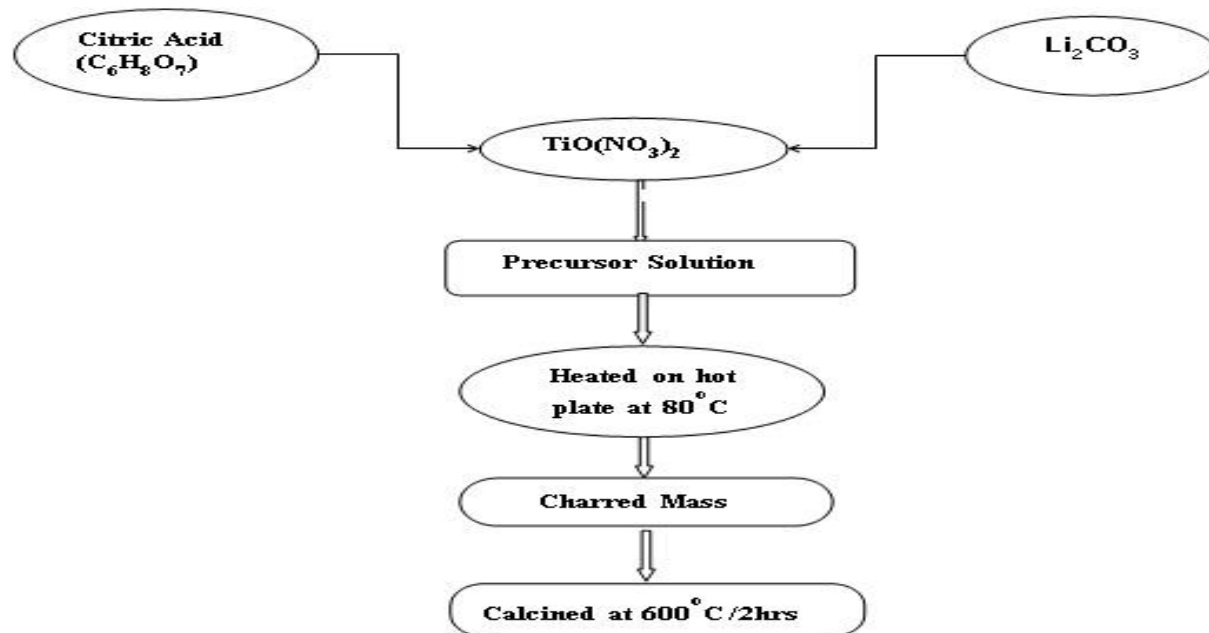


Fig. 4.2 Flow chart for preparation of Li_2TiO_3 powder.

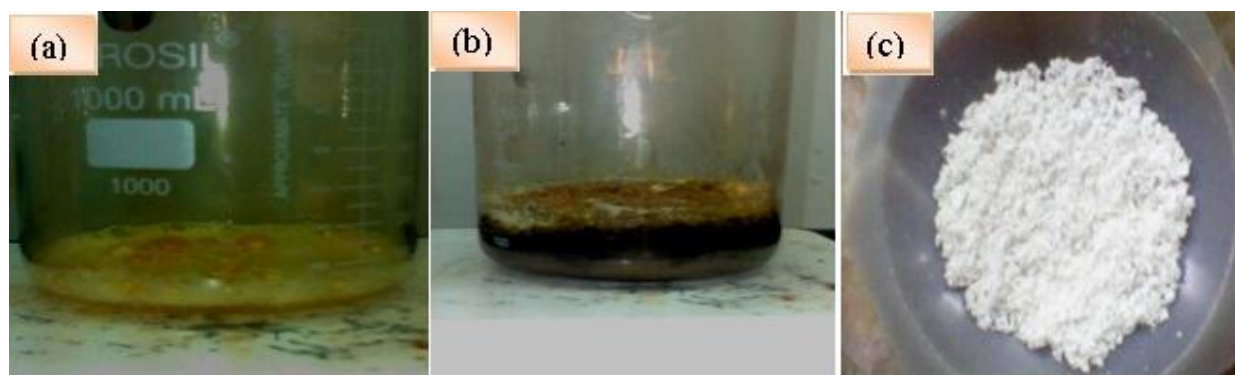


Fig. 4.3 Photographs of citrate-nitrate solution (a) pH=1

(b) auto-combustion reaction (pH=1)

(c) Calcined powder.

4.4. Powder Characterization:

4.4.1. Phase and Crystallite Size Analysis:

Phase formation of as burnt and calcined powder samples were studied by the powder X-ray diffraction performed with a Philip's Diffractometer (model: PW-1830, Philips, Netherlands) using Cu K α radiation. This technique gives some valuable information like crystal structure, crystallite size, chemical analysis etc. The generator voltage and current was set at 35KV and 25mA respectively. The scan rate was 0.04°/sec. The phases present have been identified with the search match facility available with Philips X'pert high score software.

The diffracted X-rays were detected by an electronic detector placed on the other side of the sample. To get the diffracted beams, the sample was rotated through different Bragg's angles. The goniometer keeps track of the angle (θ), and the detector records the detected X-rays in units of counts/sec and sends this information to the computer. After scanning the sample, the X-ray intensity (counts/sec) (Y axes) was plotted against the angle theta (2θ)(X-axes).

The angle (2θ) for each diffraction peak was then converted to d-spacing, using the Bragg's law;

$$n\lambda = 2d \sin\theta \quad (4.5)$$

where λ = wave length of x-ray

n = order of diffraction.

The crystallite sizes of the burnt and calcined powder samples were determined from X-ray line broadening using the Sherrer's equation [44] as follows:

$$t = 0.9\lambda / \beta \cos\theta \quad (4.6)$$

where, t is the crystallite size, λ is the wavelength of the radiation, θ is the Bragg's angle and β is the full width at half maximum.

4.4.2. Dilatometric Study:

Thermal expansion of sintered bar shaped samples was studied by NETZSCH dilatometer model DIL 402 C. In the dilatometer, the specimen is kept in a specimen holder in the center of the furnace. The linear dimensional change i.e. shrinkage or expansion of the specimen is transmitted through the push rod (pressed against the sample inside the furnace) to the measuring head.

Samples size was a bar having diameter 6 mm and length 15 mm for dilatometer experiment. The heating rate was maintained at 10°C/min. The measurement was carried out from room temperature to 1100°C in air atmosphere.

4.4.3 Preparation of Bulk Sample:

Calcined powder was mixed with 3-7 wt. % PVA (Poly Vinyl Alcohol) binder with the help of mortar and pestle. The binder mixed powder was compacted to give a desired shape for further characterization. The binder mixed powder was dried and granulated. The granules were pressed

using a hydraulic press at a pressure of 275 MPa for 2 minutes in a hydraulic press (4T, Carver Inc ,USA) to form cylindrical pellets (Dia-12.5 mm, thickness-2 mm).

4.4.4. Sintering:

Sintering of green compacts was carried out in a chamber furnace (45R5Y) by heating it from room temperature to 650°C at a heating rate of 3°C/minute with a holding time of 60 minutes at 650°C for binder removal. Thereafter, the heating was continued at the rate of 3°C/minute till the final sintering temperature was attained. A holding time was provided at the peak sintering temperature. Following the sintering, the samples were cooled in the furnace itself to room temperature.

4.4.5. Density and apparent porosity:

Bulk density and apparent porosity of sinter specimens were determined by Archimedes principle. Sintered samples were weighed in dry state. Samples were immersed in kerosene and kept under a vacuum desiccator 4 hours to ensure that kerosene filled up the open pores completely. Then, soaked and suspended weights were measured.

The apparent porosity and bulk density were calculated as follows:

W_d = Dry weight of the sample,

W_s = Soaked weight of the sample,

W_a = Suspended weight of the sample

$$\text{Bulk density} = \frac{W_d}{W_s - W_a} * \text{Density of kerosene} \quad (4.10)$$

$$\text{Apparent porosity} = \frac{W_s - W_d}{W_s - W_a} * 100 \quad (4.11)$$

4.4.8. Microstructural analysis:

Microstructural analysis is one of the important interpretation tools regarding the tritium release property of breeder material. For tritium recovery purpose, we need samples having 85-90% of TD with a significant open porosity of 5%. Again, uniform grain size distribution having diameter between 2-4 μ m is required for this purpose.

The fired and fractured surfaces were cleaned in acetone and dried at 100°C for 24hr for SEM imaging. Some sample surfaces were polished on fine emery paper; the samples were thermally etched at 50°C less than the sintering temperature. Powder samples were dispersed in water medium in ultrasonic vibrator (Oscar, Sonopros PR-1000MP). One drop was put on a glass plate and dried under IR lamp for 4 hr prior to the SEM imaging.

4.4.9. Electrical conductivity measurements:

For electrical characterization, the sintered pellets were polished by fine emery paper to make their faces smooth and parallel. Samples were painted with conducting silver paste on the parallel surfaces followed by curing at 500°C for 30 minutes. The AC resistivity ' ρ ' was calculated using the formula

$$\rho = RL/A \quad (4.12)$$

Where R= Resistivity

L= Thickness of sample

A=Area of cross section

The conductivity was calculated by taking the inverse of ρ .

The electrical conductivity follows the empirical equation given by

$$\sigma = \sigma_o \exp(-Ea/kT) \quad (4.13)$$

Where σ_o = the pre exponential factor

Ea = the activation energy,

k = Boltzmann's constant

T = Temperature in Kelvin.

CHAPTER 5

RESULTS AND DISCUSSIONS

5.1 Phase analysis:

The phase study was carried out by the X-Ray Diffraction procedure. The figure shows the relative peaks of the raw powder i.e. the powder as obtained after the auto-combustion procedure. As XRD graph shows that peaks are not sharp and broad in nature which indicates the amorphous nature of the uncalcined powder. However, after calcination at 600°C for 2 hours, the peaks become sharper and more intense which indicates the crystallinity of the powder. Also, the uncalcined powder had some carbonaceous residue which resulted in the gray color of the powder. But, after calcination at 600°C for 2 hours, this carbonaceous material was removed and a white powder was obtained and there are no secondary phase presents in the sample.

X-ray diffraction pattern identification revealed formation of monoclinic phase (JCPDS card number 33-0381) for the LT2 sample with lattice parameter $a=5.11\text{Å}$, $b=8.74\text{Å}$, $c=9.80\text{Å}$ and $\beta=100.8^\circ$ which is the same as theoretical calculations.

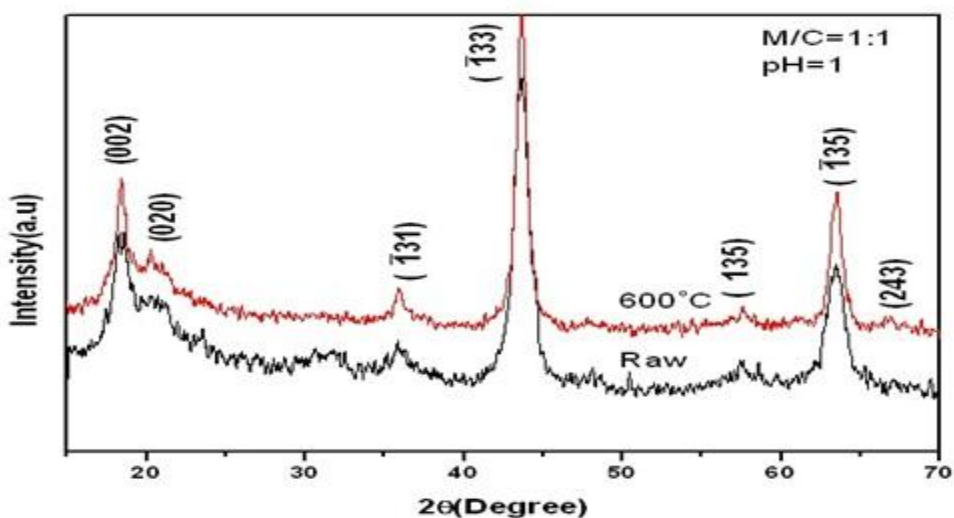


Fig. 5.1 XRD of Li_2TiO_3 with C/M=1 raw combustion powder and powder calcined (600°C)

5.2 Shrinkage Characteristics:

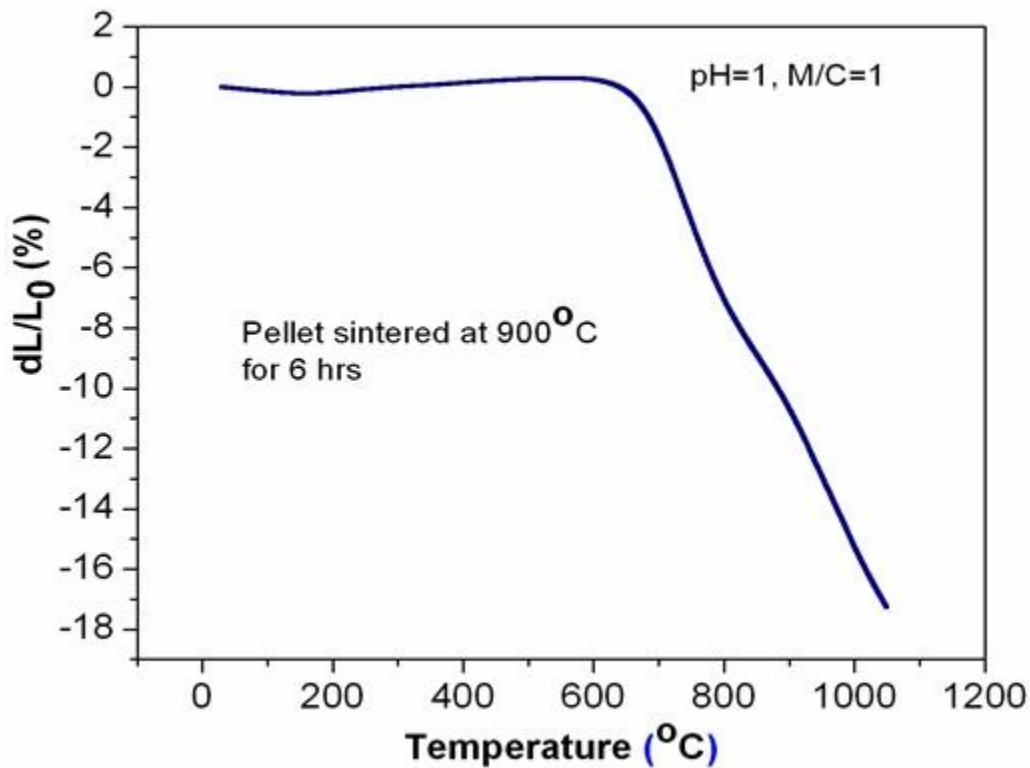


Fig. 5.2 The dilatometric shrinkage curve

Fig. 5.3 exhibited the percentage of thermal shrinkage $[(dL/L_0) * 100]$ versus temperature, where L_0 is the initial length. The plot shows that the sintering commences at a relatively lower temperature of 650 $^{\circ}\text{C}$ with a final shrinkage of around 16.5% at about 1050 $^{\circ}\text{C}$. This plot shows us that the pellets can easily be sintered at temperatures as low as 900 $^{\circ}\text{C}$ without much change in properties. However, this test needed to be stopped at around 1050 $^{\circ}\text{C}$ because of the fear that the sample may stick to the holder in the dilatometer causing problems.

5.3 Densification:

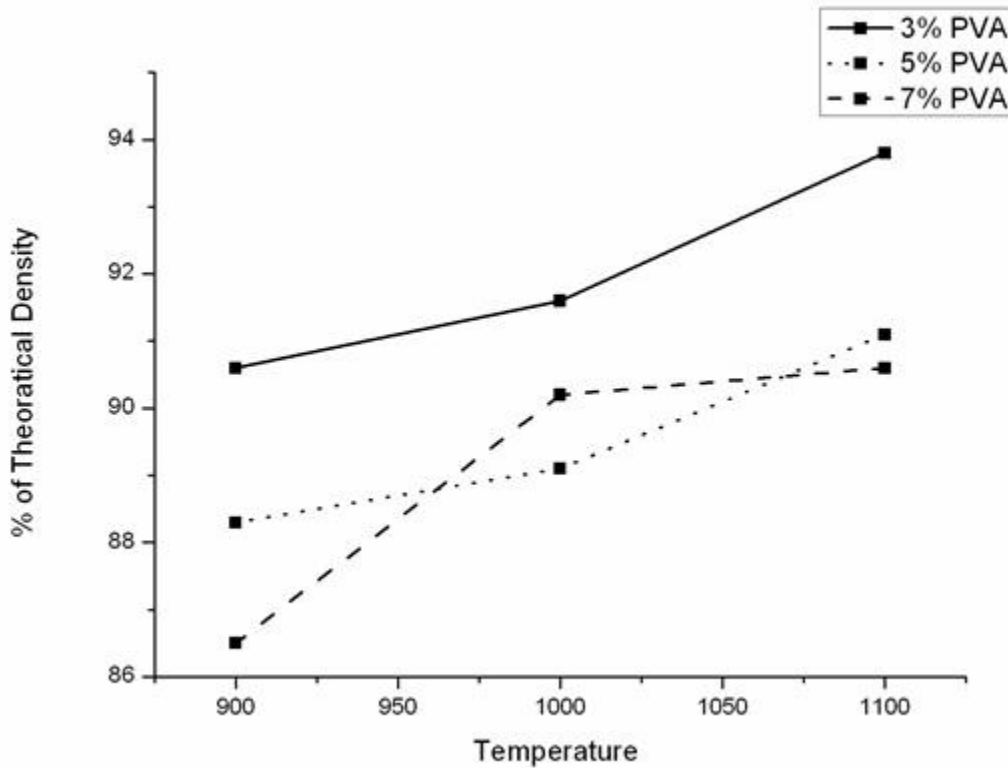


Fig. 5.3 The Bulk densities (relative) of Li_2TiO_3 at different sintering temperatures

Fig.5.3. depicts the effect of sintering temperature on the sintered density for the different samples. The relative densities of the pellets sintered at 900°C for 6 hours show about 90% of the theoretical density. It is further observed that the densities observed for 3% PVA concentration of binder is more than those observed for 5% and 7% PVA concentrations.

Also, at the higher temperatures when the soaking time is reduced, i.e. 4 hours at 1000°C and 2 hours at 1100°C , it is observed that the densities of the pellets had higher values. The idea behind reducing the soaking period is to minimize the grain growth in final stage of sintering.

5.4 Microstructures of the pellets:

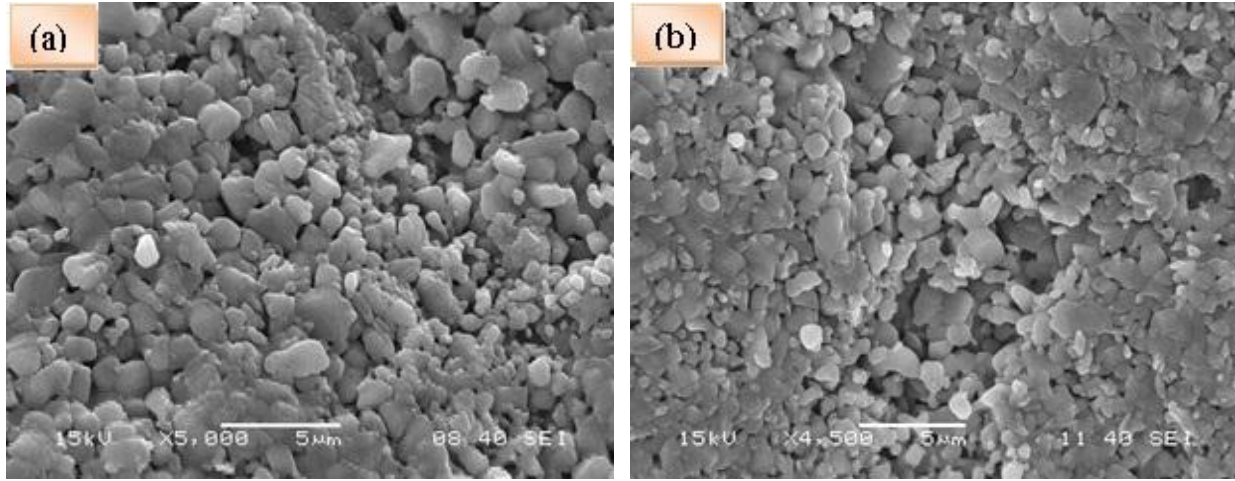


Fig.5.4 SEM micrograph of Li_2TiO_3 sintered at 900°C (a) as cut and polished surface (b) polished surface

The SEM analysis of the pellets sintered at 900°C showed some interesting characteristics. It is clearly seen that the grain size is in the order of $1\text{--}2\ \mu\text{m}$ and the presence of the closed pores is negligible. This can be attributed to the fact that the grain growth in Li_2TiO_3 is quite rapid at higher temperatures which lead to large size grains. However, for efficient tritium release, this is not required because of the simple fact that the larger the grains are the more distance the Tritium ion has to travel before coming out which is detrimental for the breeder material as large diffusion path of tritium ion results in its entrapment in the grain. Hence small grain size is required since it reduces the diffusion path and ensures release of more number of tritium. Therefore, we come to a conclusion that for better properties the sintering temperature needs to be less as well as high density pellets should be fabricated.

5.5 Thermal Expansion:

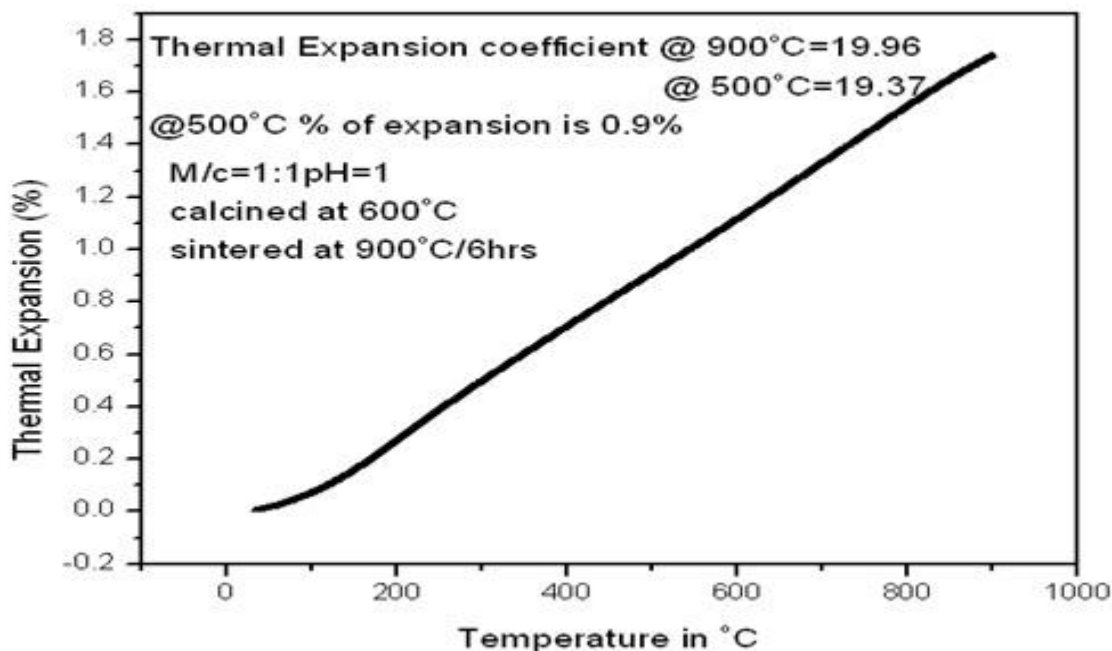


Fig. 5.5 The Thermal expansion behavior of Li_2TiO_3 pellet sintered at 900°C for 6 hours.

The thermal expansion behavior is one of the most important characteristics for materials supposed to operate at high temperatures. This is important because of the fact that expansion leads to stress which intern causes crack generation which can propagate in the structure leading to is fragility and ultimately dusting of the material. During operation of the blanket, thermal stress may arise due to the differential expansions of the bed and the structural materials.

The thermal expansion was studied in a dilatometer. The thermal expansion ($\Delta L/L_0$) % for the sample sintered at 900°C for 6 hours with 3% PVA content was found to be 0.9% which is in accordance with the literature values.

5.6 Electrical conductivity:

To effectively understand electrical response of polycrystalline materials, complex impedance formalism is commonly employed to understand electrical response of polycrystalline materials.

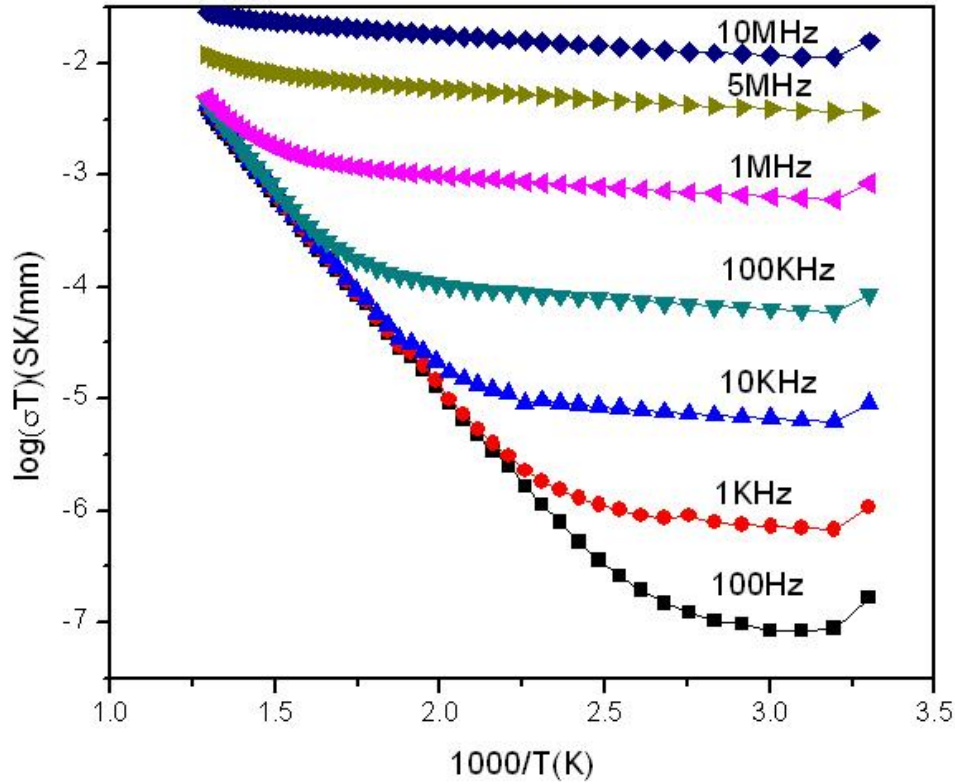


Fig.5.6 Temperature dependence of AC conductivity of Li_2TiO_3 pellets (1000°C for 4 hours)

The samples were heated from room temperature to 600°C, and the measured impedance data were converted to the specific data by taking into account the geometrical shape of the pellet.

At lower temperatures, the high frequency $\sigma_{ac}(\omega)$ is considerably higher relative to low frequency conductivity. AC conductivity is basically determined by the easiest local movement of the

charges. Also, $\sigma_{ac}(\omega)$ increases with rise in temperature which signifies that the electrical conduction in the material is a thermally activated process. However, from the conductivity plot it is seen that the conductivity dependence of temperature for the materials studied cannot be described by a single straight line which obeys the equation $\sigma T = \sigma_0 \exp(-E_a/KT)$.

CHAPTER 6

CONCLUSIONS AND SCOPE FOR FUTURE WORK

Conclusions:

- The Li_2TiO_3 powder was synthesized through the novel auto-combustion method using cheaper precursor of titanium i.e. TiO_2 . The nitrate solution was prepared by using the sulphate route and citric acid was used as the fuel. Citrate- nitrate combustion reaction was carried out to produce fine Li_2TiO_3 powders.
- It was also concluded that it can be sintered effectively at 900°C with densities of around 90% of the theoretical density.
- Different amount of PVA binder was added viz. 3%, 5%, 7% to fabricate pellets which were then sintered at different temperatures i.e. 900°C for 6 hours, 1000°C for 4 hours and 1100°C for 2 hours to produce pellets.
- The densification behavior of these pellets was studied and it was concluded that the 3% PVA pellets had the highest density among the different samples.
- The thermal expansion behavior was investigated by thermo dilatometry of sintered specimens in air atmosphere. Thermal expansion coefficient found to be around $19 \times 10^{-6}/^\circ\text{C}$.
- AC impedance method was used to characterize electrical property of the sintered sample.

Scope for future work:

- Large scale production of Li_2TiO_3 through the spray pyrolysis process.
- Pebbles formation by extruder sphredodizer.

References:

1. Benn T., 1996 *The Benn Diaries* (Arrow Books).
2. Hartley J. N., B. F. Gore and J. R. Young, *Energy* Vol. 3. (1978) P. 337-346
3. Bosch H.S et al. 1996 *Fusion* 38 415–449.
4. Johnson C.E., Hollenberg G.W., Roux N., Watanabe H., *Fusion Eng. Des.* 8, (1989), 145
5. Roux N., Avon J., Floreancig A., Mougin J., Rasneur B., Ravel S., *J. Nucl. Mater.* 233-237 (1996) 1431 – 1435
6. Lulewicz J.D., Roux N., *Fusion Eng. Des.* 39–40, (1998), 745–750
7. Wu X., Wen Z., Xu X., Gu Z., Xu X., *J. Nucl. Mater.* 373, (2008), 206–211
8. Lidsky L.M., *Nuclear Fusion*, 15, (1975), 151-173
9. Roux N., Tanaka S., Johnson C.E., Verrall R., *Fusion Eng. Des.* 41, (1998), 31–38
10. Roux N., Hollenberg G., Johnson C., Noda K., Verrall R., *Fusion Eng. Des.* 27, (1995), 154-166
11. Gierszewski P., *Fusion Eng. Des.* 39–40 (1998) 739–743
12. Miller J.M., Hamilton H.B., Sullivan J.D., *J. Nucl. Mater.* 212–215 (1994) 877
13. Kopasz J.P., Miller J.M., Johnson C.E., *J. Nucl. Mater.* 212 (1994) 927
14. Xiangwei Wu, Zhaoyin Wen, Xiaoxiong Xu, Zhonghua Gu, Xiaohe Xu, *Journal of Nuclear Materials* 373 (2008) 206–211
15. Nguyen M.H., Lee S.J., Kriven W.M., *J. Mater. Res.* 14 (1999) 3417
16. Lee S.J., Kriven W.M., *J. Am. Ceram. Soc.* 81 (1998) 2605
17. Jung C.H., Lee S.J., Kriven W.M., Ji-Yeon Park, Woo-Seog Ryu, *Journal of Nuclear Materials* 373 (2008) 194–198

18. Lee S.J., Characteristics of lithium titanate fabricated by an organic-inorganic solution route, *Journal of Ceramic Processing Research*. Vol. 9, No. 1, pp. 64~67 (2008)
19. Xiangwei Wu, Zhaoyin Wen, Xiaoxiong Xu, Zhonghua Gu, Xiaohe Xu, *Journal of Nuclear Materials* 373 (2008) 206–211
20. Xiangwei Wu, Zhaoyin Wen , Bin Lin, Xiaogang Xu *Materials Letters* 62 (2008) 837–839
21. Mohammadi M. R., Fray D. J., *J Sol-Gel Sci Technol* 2010
22. Nguyen M.H., Lee S.J., Kriven W.M., *J. Mater. Res.* 14 (1999) 3417
23. Sinha A., Nair S.R., Sinha P.K., *Journal of Nuclear Materials* 399 (2010) 162–166
24. Jung C.H., Park J.Y., Oh S.J., Park H.K., Kim Y.S., Kim D.K., Kim J.H., *Journal of Nuclear Materials* 253,(1998),203–212
25. Jung C.H, Lee S.J, Kriven W. M., Ji-Yeon Park , Woo-Seog Ryu, *Journal of Nuclear Materials* 373 (2008) 194–198
26. Cruz D., Pfeiffer H., Bulbulian S., Synthesis of Li_2MO_3 ($M = \text{Ti}$ or Zr) by the combustion method, *Solid State Sciences* 8 (2006) 470–475
27. Song J.H., Evans J.R.G., A dry pressing strength for test of agglomerate strength, *J. Am. Ceram. Soc.* 1994 3(77), 806-814.
28. Baklouti S., Chartier T., Baumard J.F., Mechanical properties of dry pressed ceramic green products; the effect of binder, *J. Am. Ceram. Soc.*, 1997, 80(8), 1992-1995.
29. Youschaw R.A., Holloran J.W., compaction of ceramic dried powder, *Am. Cer. Bull.*, 1982, 61(2), 227-230. Song J.H., Evans J.R.G., A dry pressing strength for test of agglomerate strength, *J. Am. Ceram. Soc.* 1994 3(77), 806-814.
30. Wang J. Effect of pressing method on organic burnout, *J. Am. Ceram. Soc.* 1992, 75(9), 2627-2629

31. Reed J.S., Introduction to the principles of ceramic processing, John Wiley and Sons, New York, 1988
32. Dunn A.S., Coley R.L., Duncalf B., Thermal decomposition of poly vinyl alcohol, In properties and applications of Poly vinyl alcohol, Society of Chemical Industries (SCI), London, 1968, pp. 208-221
33. Dong, C. and Bowen, H.K., Hot-stage study of bubble formation during binder burnout, *J. Am. Ceram. Soc.*, 72, 1082, 1089
34. Masia, S., Calvert, P.D., Rhine, W.E., and Bowen, H.K., Effect of oxides on binder burnout during ceramics processing, *J. Mater. Sci.*, 24, 1907, 1989.
35. Lang G., Zeitschrift für Anorganische und Allgemeine Chemie 276, (1954), 7
36. Hodeau J. L., Marezio M., *Journal Of Solid State Chemistry* 45, (1982), 170-179
37. Dorrian J.F. and Newnham R.E., *Mat. Res. Bull.* 4 (1969) 179.
38. Fehr Th., Schmidbauer E., *Solid State Ionics* 178 (2007) 35–41
39. Noda K., Ishii Y., Matsui H., Ohno H., Hirano S. and Watanabe H., *Journal of Nuclear Material* 155- 157 (1988) 568-571
40. Davis J.W., Haasz A.A., *Journal of Nuclear Materials* 232 (1996) 65-68
41. Saito S., Tsuchiya K., Kawamura H., Terai T., Tanaka S., *Journal of Nuclear Materials* 253 (1998) 213–218
42. Abou-Sena A., Ying A., Abdou M., Experimental measurements of the effective thermal conductivity of a lithium titanate (Li_2TiO_3) pebbles-packed bed, *Journal of Materials Processing Technology* 181 (2007) 206–212
43. J. Tsay and T. Fang, *J. Am. Ceram. Soc.*, 1999, 82, 1409
44. B. D. Cullity, 'Elements of X-Ray Diffraction', 2nd Ed, Addison-Wesley, INC (1978).

